Transition from tunneling to direct contact in tungsten nanojunctions

A. Halbritter, Sz. Csonka, and G. Mihály
Electron Transport Research Group of the Hungarian Academy of Science at Budapest University of Technology and Economics, 1111 Budapest, Hungary

E. Jurdik, O. Yu. Kolesnychenko, O. I. Shklyarevskii,* S. Speller, and H. van Kempen
NSRIM, University of Nijmegen, Toernooiveld 1, 6525 ED Nijmegen, the Netherlands
(Received 11 January 2003; published 17 July 2003)

We apply the mechanically controllable break junctions technique to investigate the transition from tunneling to direct contact in tungsten. This transition is quite different from that of other metals and is determined by the local electronic properties of the tungsten surface and the relief of the electrodes at the point of their closest proximity. When flat surfaces approach each other, an avalanchelike jump to direct contact occurs at anomalously large distances $z \approx 3-5$ Å. In contrast, ballistic contact between irregularly shaped electrodes is established without discontinuity in conductance curves, indicating the absence of spontaneous formation of an adhesive neck. Conductance histograms of tungsten are either featureless or show two distinct peaks related to the sequential opening of spatially separated groups of conductance channels. The role of surface states of tungsten and their contribution to the junction conductance at sub-Å electrode separations are discussed.

DOI: 10.1103/PhysRevB.68.035417 PACS number(s): 73.40.Jn, 72.15.−v

I. INTRODUCTION

The study of transition from tunneling to direct contact and electrical transport through atomic-sized metallic conductors has been the object of great attention during the last decade. Different types of phenomena, related to both the quantum character of transport and the atomic discreteness of the contact, were observed in 3D nanoconstrictions produced by scanning tunneling microscopes (STM) or mechanically controllable break junctions (MCBJ's).[1] In particular, conductance measurements of breaking nanowires demonstrated a steplike structure of conductance versus electrode separation traces $G(z)$. For single-valence *s*-metal conductance plateaus are close to the integer multiples of the quantum conductance unit $G_0 = 2e^2/h$. However, simultaneous measurements of both the force and the conductance for breaking gold nanowires demonstrated that jumps between plateaus in the conductance staircase are always correlated with relaxations of the mechanical force and, therefore, with atomic rearrangements in the nanoconstriction.[2] Individual conductance curves $G(z)$ are inherently irreproducible due to the different dynamical evolution of the connective necks during the break. Therefore, analysis of experimental data includes construction of conductance histograms based on a large number of conductance traces. Peaks in the conductance histograms are related to the statistically more probable atomic configurations in the connective neck between the electrodes.[3] For polyvalent metals the main (and sometimes the only) feature in the conductance histograms is a peak corresponding to one-atom point contact.[4] The conductance through such a contact is determined by a few conductance channels intimately related to atomic orbitals.[5] Transition from tunneling to single-atom contact occurs in an avalanchelike way at an electrode separation of ~ 1.5 Å due to the metallic adhesion forces.[6] This sudden jump in conductance precluded measurements of $G(z)$ at sub-Å distances between the electrodes for all metals studied to date.

While measuring thermal expansion of MCBJ electrodes for different materials, we took notice of the unusually high stability of tungsten tunnel junctions at very close electrode separations.[7] In another study, transmission and scanning electron microscopy images showed no evidence of connective neck formation between tungsten wires.[8] Moreover, measurements of adhesive forces between an atomically-defined W(111) trimer tip and a Au(111) sample revealed no spontaneous jump to contact.[9] These unusual properties of tungsten nanocontacts motivated us to carry out further extensive investigations.

In this paper we present our experiments with tungsten MCBJ. Our aim was to examine the behavior of tungsten nanojunctions during the transition from tunneling to direct contact and to what extend this behavior is influenced by the unique mechanical and electronic properties of tungsten. We show that very often the adhesive jumps of conductance are absent and that the transition to single atom contact is smooth. This permitted us to investigate the junction at unprecedented ultrasmall electrode separations. By employing the conductance histogram technique we determined the preferential values of conductance during the fracture of the junction to be about $1G_0$ and $2G_0$. We show that the special evolution of the conductance in tungsten junctions is mostly governed by the extreme hardness of the contact and by surface electronic states at the W(001) surface that occasionally terminates the junction electrodes. Also, we measured the conductance histograms of tantalum and molybdenum (as the two nearest neighbors of tungsten in the periodic table of elements) to provide additional support for our model.

II. EXPERIMENTAL SETUP

We employed the traditional MCBJ technique, described elsewhere,[1] with a modified sample mounting (Fig. 1). This mounting includes two $6 \times 2.5 \times 1$ mm pieces of shear piezoceramic (which gives horizontal displacement of its surface

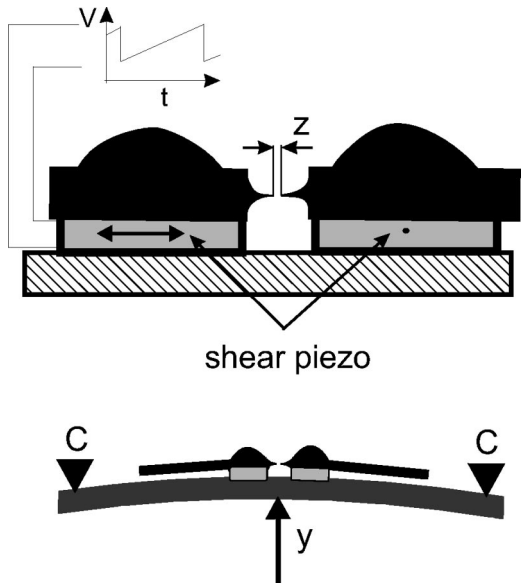

FIG. 1. Modified sample mounting. The tungsten wire is glued on top of shear piezoceramic attached to a phosphor bronze bending beam. The distance between the electrodes is controlled by vertically pushing the bending beam at the middle or by applying voltage on the left-hand side shear piezo. All distances are exaggerated for clarity.

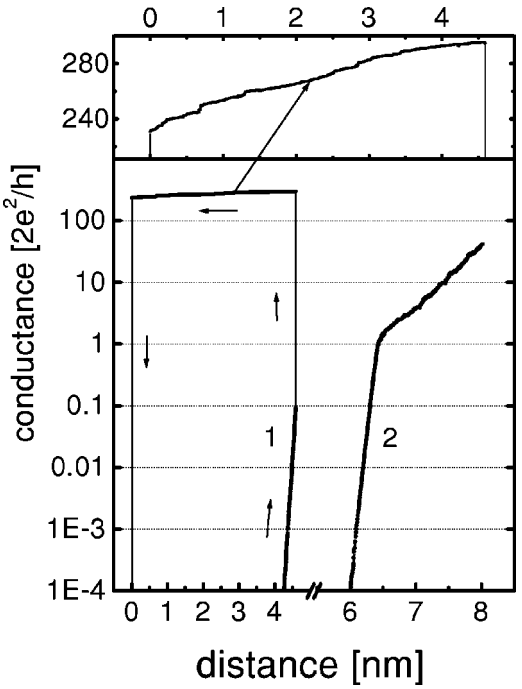

FIG. 2. Two extreme cases of $G(z)$ traces for W MCBJ. 1: Avalanchelike transition from tunneling to a low-Ohmic contact. The upper panel shows the contact conductance in the process of retraction. 2: Transition from tunneling to direct contact without spontaneous formation of an adhesive neck.

when voltage is applied) glued at the center of a phosphor bronze bending beam. A polycrystalline tungsten wire with a diameter of 100 μm was attached to the top of the piezo's with two small drops of hard epoxy (Stycast 850FT). The central section of the wire was then electrochemically etched in a 25% solution of KOH down to 5–10 μm at its thinnest part. The wire was broken at 4.2 K in an ultrahigh vacuum environment by bending the beam. The distance between the electrodes was fine tuned by changing the deflection of the bending beam or applying voltage to the left-hand side shear piezo. The relative displacement of the electrodes was calibrated using the exponential part of $G(z)$ traces in the tunneling regime (assuming a work function for tungsten $\phi \simeq 4.5$ eV) as well as by measuring field emission resonance spectra.[10] The contact conductance was measured using a current-to-voltage converter with a gain of 0.1 V/μA. Conductance versus electrode separation traces $G(z)$ were measured in a slow mode (2–30 points/s) using Keithley 2182 nanovoltmeters in order to cover over 7 orders of magnitude in the conductance during transition from tunneling to direct contact. Conductance traces for building conductance histograms were recorded with an AT-MIO-16XE-50 National Instruments data acquisition board (sampling rate of 20 000 points/s and resolution of 16 bits). During this acquisition a ramp voltage with a frequency of 5–50 Hz was applied to the shear piezo to establish a repeated fracture of the junction.

The electrode surfaces were characterized using different methods. By linear scan with the two shear piezo's in the constant current mode we found atomically flat parts of the surface up to 5–10 nm in length alternated with irregularities of 5–15 Å in height. It should be noted that these STM-like measurements with two ''blunt'' electrodes are rather qualitative and the numbers presented are only rough estimates. On many occasions, we also found that the distance versus voltage curves $S(V)$ measured in the constant current are linear up to a bias voltage of $\pm$35–40 V (Fowler-Nordheim regime of tunneling). This means that the radius of curvature for both electrodes is essentially larger than 100 nm.[11] In such cases we were able to study stable tunnel junctions with feedback currents as high as 50–100 μA for a bias voltage down to 0.4–0.5 V (tunneling regime) and, therefore, with very high tunnel conductance. When an electrode separation of $\sim$3 Å is assumed, the electrodes are atomically flat at least over an area of 5–10 nm^2. We analyzed thoroughly more than 200 conductance histograms measured for 12 different samples.

III. RESULTS

We investigated the transition from the tunneling regime to direct contact for tungsten MCBJ by performing conductance measurements during slow, continuous approach or retraction of the electrodes. These measurements revealed a rich variety of $G(z)$ traces. All of them fall between two extreme cases shown in Fig. 2. Curve 1 demonstrates an avalanchelike transition from $G \approx 0.01$–$0.1 G_0$ to 100–$1000 G_0$. This indicates the formation of a mesoscopic contact with a cross section of 10–100 nm^2 between two atomically flat portions of the electrodes. From the amplitude of conductance jumps we estimated that these spontaneous transitions occur at interelectrode separations $\gtrsim 3$ Å. Subsequent retraction of the electrodes produced only small changes in the contact conductance over a retreat distance of

$\gtrsim 4$ nm, which were followed by sudden disconnection (upper panel in Fig. 2). During 5–10 min after disconnection, the distance between the electrodes increased as deduced from the transient decrease of the measured tunnel current. This effect is related to a gradual relaxation of the overstretched part of electrodes and was observed earlier on a considerably longer time/distance scale following the initial break of other metallic wires.[12] After the full relaxation of the sample, the original curve could be reproduced accurately, indicating that no irreversible changes of the electrode relief occurred. The other extreme case—curve 2 in Fig. 2—demonstrates a smooth transition from tunneling to direct contact with no sign of spontaneous formation of an adhesive neck. This case most likely corresponds to contacts between irregularly shaped parts (e.g., asperities or edges of facets) of the electrode surfaces. However, the majority of $G(z)$ curves exhibited combination of smooth changes of the conductance and sudden jumps with amplitudes ranging from $0.1G_0$ up to few G_0.

We also performed statistical analysis of conductance traces by employing the conductance histogram technique. We found that tungsten nanojunctions have a particular tendency to show reproducible, almost identical conductance traces when indentation of the electrodes is not sufficient. If proper care is exercised and in every cycle contacts of $G \gtrsim 30-40G_0$ are formed, the break occurs in a large variety of ways. Only then, a statistical approach to data analysis is justified. In sharp contrast to other metals, the conductance histograms of tungsten do not necessarily exhibit the same pattern when the contact site is shifted by the right-hand side shear piezo or when the sample is replaced. A major part of histograms demonstrated no distinctive features [Fig. 3(a)]. However, on many occasions the histograms showed two peaks at respectively 1–1.2 and $2-2.2G_0$ [Fig. 3(b)], or only one of those two.

In Fig. 4 four characteristic conductance traces are presented. Curve 1 shows a smooth and completely featureless transition from direct contact to tunneling. For a tungsten junction this kind of transition is frequently present and gives rise to the featureless background in the conductance histograms. This background is suppressed when these featureless curves are rejected from the data set by employing a computer filtering algorithm.[13] Then, either peaks invisible in the original histogram appear [inset in Fig. 3(a)] or the contrast of peaks is significantly improved [inset in Fig. 3(b)]. Peaks in the histogram naturally arise from conductance traces with distinct features—plateaus—at about $1G_0$ and/or $2G_0$ as demonstrated by curves 2, 3a, and 3b in Fig. 4. While curve 2 shows a smooth transition with no jumps, in the case of curves 3a and 3b clear jumps occur near $1G_0$ and $2G_0$, respectively. We note here that conductance traces like those represented by curve 2 are unique to tungsten and were not observed in other metallic contacts.

In our previous analysis we used an algorithm to select the traces with long plateaus.[13] However, it is also important to differentiate between the smooth curves and those with sudden jumps. For this reason every trace was characterized by the largest jump between neighboring data points in the conductance interval $G/G_0 \in [0.3,3.3]$. By combining these two approaches the traces were classified into the three categories presented in Fig. 4. Using the data set for histogram in Fig. 3(b) we found that $\sim 30\%$ of traces exhibited a smooth and featureless transition and roughly 10% of curves show plateaus without sudden jumps. In the rest of the traces clear conductance jumps were found. In order to quantify at which conductance values conductance jumps with $\Delta G_{\max} \geqslant 0.7G_0$ are most likely to occur, we also built up histograms for the position of these sudden transitions. The peaks in the so-built histogram presented in Fig. 5 clearly demonstrate that large conductance jumps are most probable at $G \simeq 1G_0$ and $2G_0$. We emphasize that the relative occurrence of the three different types of conductance traces is sample and site-dependent, and in certain data sets only traces with smooth transitions were present.

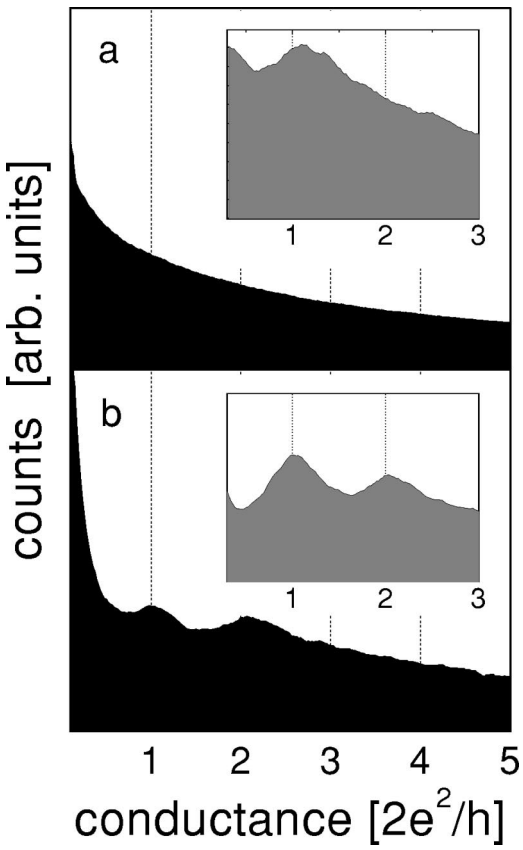

FIG. 3. Conductance histograms for W MCBJ based on $10\,000G(z)$ traces. (a) Featureless histogram. (b) Histogram with peaks close to integers of $2e^2/h$. Insets in (a) and (b): histograms for the corresponding data sets after filtering out the featureless curves.

IV. DISCUSSION

Our experimental results for tungsten nanojunctions strikingly differ from those obtained for other metals studied so far, that exhibit conductance traces always falling into the same (material-specific) pattern. Especially, the adhesive jump to contact or the tensile overstretching followed by sudden disruption have respectively been found to be an unavoidable attendant of contact formation or breakage. This

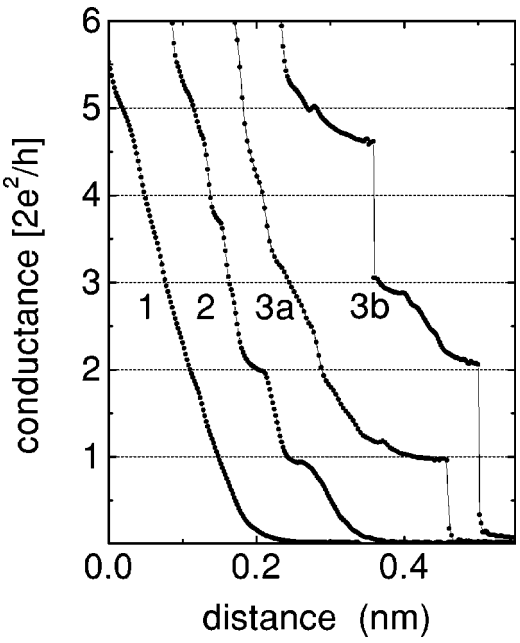

FIG. 4. Typical conductance traces for W. Curve 1: featureless curve. Curve 2: smooth transition to tunneling with distinct plateaus. Curves 3a and 3b: traces with sudden jumps of conductance.

has precluded measurements of conductance at small electrode separations. The occasional absence of these processes is unique for tungsten junctions and we attribute it to the specific mechanical properties of this metal. In particular, this odd junction stability at ultrasmall electrode separations permitted us to study the previously unaccessible regime of nanocontact conductance.

The adhesive jump is governed by the competition between the adhesive and tensile forces.[14] The tensile forces

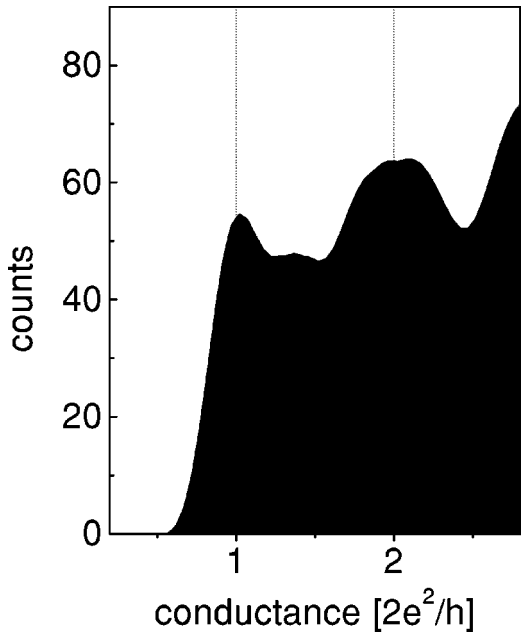

FIG. 5. Histogram for conductance values at which jumps with amplitude $\Delta G > 0.7 G_0$ occur.

are determined by the stiffness of the electrodes, which is composed of the stiffness of the nanoscale junction itself and the stiffness of the whole setup. The latter can have significant importance in an atomic force microscope with a soft cantilever, however, it is not expected to play any role in an MCBJ due to the rigid sample mounting. The stiffness of the junction depends on the strength of the bonds in the material, but also the junction geometry and the crystallographic orientation of the electrodes have a crucial influence on it. Contacts with a large opening angle have large stiffness, while in contacts with a small opening angle a large amount of layers are involved in the elastic deformation and thus the stiffness is reduced. The stiffness is also reduced when the contact surfaces are not perpendicular to the contact axis. Then, the electrodes can bend similar to a cantilever and the elastic behavior is defined by the smaller shear forces.

The elastic behavior of the material is basically determined by the strength of the bonds between the atoms. Therefore it is similar for all lengthscales and atomic scale systems are well described by the bulk elastic constants.[2] The bulk elastic modulus of tungsten ($E_W = 411$ GPa) is outstandingly large among all metals. (For comparison the Young module of Au, Pt, and Nb are $E_{Au} = 78$ GPa, $E_{Pt} = 168$ GPa, and $E_{Nb} = 105$ GPa.) On the other hand, the junction geometry is not controllable in MCBJ experiments. In previously studied metals the conductance traces imply that the junction breaks through the process of rupture. In this case the contact geometry is ''self-organized'' during the neck pulling, so the conditions for adhesive jumps are similar during each disconnection. Our measurements imply that tungsten breaks in a more brittle way and a large variety of contact geometries are established during the fractures. This, together with the outstanding elastic modulus of tungsten can explain our observations. In ''stiff'' contact geometries the elastic forces can overcome the adhesion and thereby enable a smooth transition between tunneling and direct contact. In softer contact geometries the adhesive jumps are still present.

Our interpretation can be tested by comparing the mechanical behavior during the break of further metals with different elastic module. For this reason we performed measurements on two neighbors of tungsten in the periodic system: molybdenum and tantalum. These metals have similar electronic properties to tungsten. The elastic modulus of molybdenum is relatively large ($E_{Mo} = 329$ GPa), while tantalum is much softer ($E_{Ta} = 186$ GPa). In agreement with that we found that tantalum always breaks in a jumplike way, while in molybdenum a part of the conductance traces showed a smooth transition.

To explain the avalanchelike motion of hundreds of atoms in the extreme case presented in Fig. 2 as curve 1, we consider the following three possibilities. The first one corresponds to the motion of a number of atomic layers in the direction normal to the electrode surfaces as assumed in the calculations by Taylor *et al.*[14] This possibility would require an avalanche of a macroscopic amount of metal. Such a situation can take place only for contacts that act as a very soft spring and thus we do not consider it as the most likely explanation. The second possibility, that would result in the same behavior of the contact conductance, is the transition to

direct contact due to bending of the electrodes. This arrangement is likely to occur when flat parts of the electrode surfaces are not perpendicular to the electrode axis. Then, the component of the adhesive force that is normal to the electrode axis causes bending. During our experiments, we observed anomalously high sensitivity of the tungsten MCBJ to acoustic vibrations, such as human voice, that suggests a transverse, springlike motion of the electrodes. This observation is in favor of the ''bending model.'' As the last possibility, the contact between the electrodes may emerge as a result of dislocation glide or homogeneous shear motion of one of the electrodes.[1] However, in this case it is not possible to explain the reversible behavior of contact conductance through many formation-breaking cycles.

The smooth conductance traces with plateaus at the first two conductance quanta (e.g., curve 2 in Fig. 4) are very close to those expected for conductance quantization in short constrictions.[15] In spite of its attractiveness, we discarded this effect as the possible origin of the peaks in our histograms. Extremely small distances between the plateaus in conductance traces of tungsten $\Delta z \simeq 30$ pm, suggest a constriction with an opening angle close to 90° (an orifice). In this case the conductance quantization must be completely suppressed.[15] The shape of these traces is better explained by the sequential opening of conduction channels due to different spatial distribution of the involved electronic states.

For transition *d*-metals five conductance channels are expected to contribute to the conductance of a single-atom contact according to the number of valence orbitals. The transmission values of these conductance channels were extensively studied for single-atom niobium junctions by tight binding calculations[5] and by measuring subgap structure in the superconducting state.[16] The calculations performed for a simplified one-atom contact geometry revealed a single dominant channel (as a result of the hybridization between the *s* and d_{z^2} orbitals), two medium-sized channels and two smaller channels that yield together a net conductance of $G=2-3G_0$. Both the conductance and the transmission coefficients showed a good agreement with the values determined from the experiment. For all nonmagnetic transition metals studied so far (Nb, V, Rh, Pd, Ir, Pt) the histograms show a single well-defined peak centered in the region of $G=1.5-2.5G_0$, that is attributed to the conductance through a single-atom contact.[1,4] To date, theoretical calculations have not been performed for the conductance of a single-atom tungsten contact, but its value is assumably in the same range $G \simeq 1.5-2.5G_0$.

As tungsten is the most extensively used material for STM-tips numerous efforts have been made to understand the nature of its localized surface states and their role in achieving atomic resolution. First principle calculations for the W(001) surface demonstrated that the tunnel current is primarily generated by the $5d_{z^2}$ dangling-bond surface states.[17,18] At distances >2 Å from nuclei the charge density of the surface state is much higher than that of the atomic $6s$ state[19] and, therefore, surface states play a key role in the electron transport at small separations. The break of tungsten crystals occurs preferentially along the W(001) plane[20] and there is a high probability that at least some facets at the MCBJ electrode surface are oriented in this (001) direction.

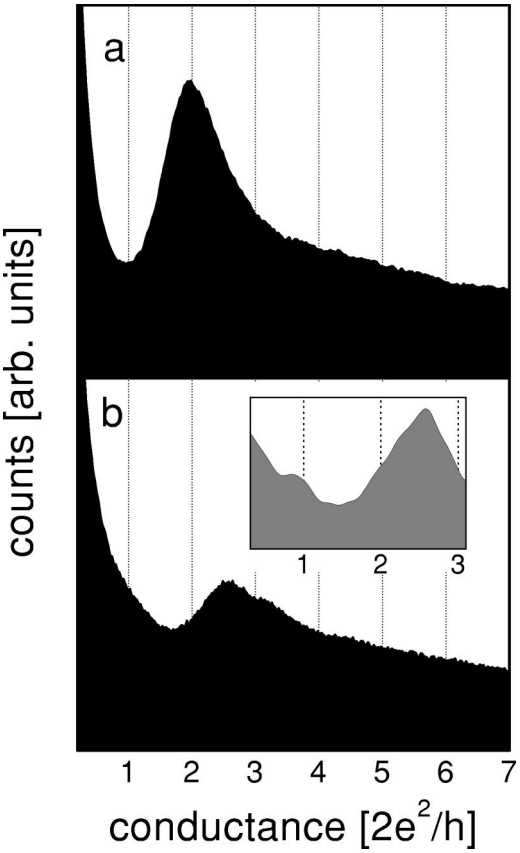

FIG. 6. Conductance histograms for tantalum (a) and molybdenum (b) based on 20000 conductance traces. Inset in (b) shows a histogram for selected 10% of the curves, exhibiting plateaus around $1G_0$.

We can therefore argue that the plateau at $2G_0$ is due to the conductance through atomic valence orbitals in a one-atom contact geometry. Then, the plateau at $1G_0$ is connected to a single conduction channel through a dangling-bond surface state at electrode separations, where the contribution of other channels becomes small. The absence of adhesive jump-to-contact enables us to monitor the transition between both these situations. Such a sequential overlap of spatially separated groups of conductance channels may only occur for specific electrode configurations when the foremost atom of the ''tip'' electrode approaches the top site of the ''sample'' electrode. This explains the relatively low percentage of $G(z)$ traces with distinct plateaus. Conductance traces such as the curves 3a and 3b in Fig. 4 also contribute to the peaks observed in the conductance histograms. In this case, however, the adhesive jump is not suppressed and, therefore, the elastic overstretching of a certain configuration followed by its sudden relaxation is observed instead of a smooth transition. In spite of that, the position of the plateaus can be explained using the same argumentation.

In order to get further support of the model proposed, we investigated the conductance of tantalum and molybdenum quantum contacts. These *d* metals with bcc lattice are the nearest neighbors of W in the periodic table. The electronic properties of both Mo and Ta are similar to tungsten. On the

other hand the hardness of Mo suggests a similar mechanical behavior to tungsten whereas the hardness of Ta is significantly smaller. The conductance histogram for Ta is presented in Fig. 6(a). It exhibits a broad, well-defined peak at $G \simeq 2G_0$. The individual conductance traces showed a pattern typical for the rest of the metals with unavoidable jumplike transition to tunneling. The conductance histogram for Mo is shown in Fig. 6(b). It exhibits a broad peak at $G \simeq 2.5G_0$ superimposed on a featureless background. The occurrence of smooth conductance traces is significantly less frequent than for tungsten and raw data show no sign for a peak around $1G_0$ in the histogram. However, in some cases computer filtering of original data sets[13] reveals conductance traces with plateaus close to the conductance quantum, and accordingly a peak around $1G_0$ is recovered in the histogram [see inset in Fig. 6(b)]. Similarly to tungsten, this feature can be explained by localized electronic states on the Mo(001) surface.[21]

The existence of the surface electronic states at tungsten surfaces can also explain that the avalanchelike transition from tunneling to direct contact occurs at distances larger than those expected for Au, Cu, and Ni surfaces[14] (see curve 1 in Fig. 2). If both of the MCBJ electrode surfaces are flat and oriented along the W(001) plane (with electronic properties dominated by the slowly decaying $5d_{z^2}$ dangling-bond surface states), one can expect a significant overlap of the electronic densities. Consequently, an adhesive avalanche at relatively large separations takes place. This result correlates with Ref. 9 in which strong attractive forces between a W tip and a Au surface were found at anomalously large distances. In addition, a similar behavior of $G(z)$ was found for a single-crystal chromium MCBJ with surfaces of electrodes oriented along the (001) direction.[22] In that case, the electronic properties of chromium are also dominated by surface states.

V. CONCLUSIONS

In conclusion, we have presented experimental evidences that the transition from vacuum tunneling to point-contact with direct conductance in tungsten MCBJ is controlled by both the electrode relief and the electronic properties of the tungsten surface. In the case of atomically flat electrodes an avalanchelike transition to direct contact occurs at anomalously large separations due to the strong adhesive forces related to the existence of the surface electronic states. Ballistic contact between irregularly shaped electrodes may occur without spontaneous formation of an adhesive neck. This provided us with the unprecedented possibility to study the junction conductance at sub-Å distances between the electrodes. Peaks in conductance histograms arise due to spatial separation of conductance channels and indicate a dominant role of the surface states in electron transport at ultrasmall distances. We would like to note here, that the very recent molecular dynamics simulations for polycrystalline sample of W also shown no one-atom neck when the nanocontact is formed along a grain boundary.[23]

The limitations of MCBJ technique precluded us from drawing a more exact and persuasive conclusion. The current data can greatly be improved by simultaneous measurements of the conductance and the forces in the course of electrode approach for contacts with a well-defined tip/sample shape and orientation. To our opinion, the details of the process of avalanchelike transition to direct contact and subsequent break can be visualized with a high resolution transmission electron microscope operating in UHV.

ACKNOWLEDGMENTS

The authors are grateful to A.J. Toonen, J. Hermsen, and J. Gerritsen for invaluable technical assistance, J.H.A.Hagelaar and J.M.Wulveryck for stimulating discussions. Part of this work was supported by the Stichting voor Fundamenteel Onderzoek der Materie (FOM) which is financially supported by the Nederlandse Organisatie voor Wetenschappelijk Onderzoek (NWO). The Hungarian Research Funds No. OTKA TO37451, TS040878, N31769 and a NWO grant for Dutch-Hungarian cooperation are also acknowledged. O.I.S. wishes to thank the NWO for a visitor's grant.

*Also at B. Verkin Institute for Low Temperature Physics & Engineering, National Academy of Science of Ukraine, 47 Lenin Ave., 61164, Kharkov, Ukraine.

[1] J.M. van Ruitenbeek, in *Metal Cluster on Surfaces: Structure, Quantum Properties, Physical Chemistry*, edited by K.H. Meiwes-Broer (Springer-Verlag, Heidelberg, 2000), pp. 175–210; N. Agrait, A. Levy Yeyati, and J.M. van Ruitenbeek, Phys. Rep. (to be published).

[2] G. Rubio, N. Agrait, and S. Viera, Phys. Rev. Lett. **76**, 2302 (1995).

[3] J.M. Krans, J.M. van Ruitenbeek, V.V. Fisun, I.K. Yanson, and L.J. de Jongh, Nature (London) **375**, 767 (1995).

[4] A.I. Yanson, Ph.D. thesis, University of Leiden, 2001.

[5] J.C. Cuevas, A. Levy Yeyati, and A. Martín-Rodero, Phys. Rev. Lett. **80**, 1066 (1998).

[6] A.P. Sutton and J.B. Pethica, J. Phys.: Condens. Matter **2**, 5317 (1990); U. Landman, W.D. Luedtke, N.A. Burnham, and R. Colton, Science **248**, 454 (1990).

[7] O.Yu. Kolesnychenko, A.J. Toonen, O.I. Shklyarevskii, and H. van Kempen, Appl. Phys. Lett. **79**, 2707 (2001).

[8] A. Correia, M.I. Marqués, and N. García, J. Vac. Sci. Technol. B **15**, 548 (1997).

[9] G. Cross, A. Schirmeisen, A. Stalder, P. Grütter, M. Tschudy, and U. Dürig, Phys. Rev. Lett. **80**, 4685 (1998).

[10] O.Yu. Kolesnychenko, O.I. Shklyarevskii, and H. van Kempen, Rev. Sci. Instrum. **70**, 1442 (1999).

[11] J.M. Pitarke, F. Flores, and P.M. Echenique, Surf. Sci. **234**, 1 (1990).

[12] R.J.P. Keijsers, J. Voets, O.I. Shklyarevskii, and H. van Kempen, Low Temp. Phys. **24**, 970 (1998).

[13] The integral $\int(|\partial_z G(z)|+\varepsilon)^{-1}dz$, where $\varepsilon>0$ is a small number used to prevent singularities, was calculated for each conductance trace within an interval $G(z)/G_0 \in [0.3,3.3]$ and its value was used to select the curves with distinct plateaus.

[14] P.A. Taylor, J.S. Nelson, and B.W. Dodson, Phys. Rev. B **44**, 5834 (1991).
[15] J.A. Torres, J.I. Pascual, and J.J. Saenz, Phys. Rev. B **49**, 16 581 (1994).
[16] B. Ludoph, N. van der Post, E.N. Bratus, E.V. Bezuglyi, V.S. Shumeiko, G. Wendin, and J.M. van Ruitenbeek, Phys. Rev. B **61**, 8561 (2000).
[17] S. Ohnishi and M. Tsukuda, Solid State Commun. **71**, 391 (1989).
[18] C.J. Chen, Phys. Rev. B **42**, 8841 (1990).
[19] M. Posternak, H. Krakauer, A.J. Freeman, and D.D. Koeling, Phys. Rev. B **21**, 5601 (1980).
[20] J. Riedle, P. Gumbsch, and H.F. Fischmeister, Phys. Rev. Lett. **76**, 3594 (1996).
[21] S.B. Legoas, A.A. Araujo, B. Laks, A.B. Klautau, and S. Frota-Pessôa, Phys. Rev. B **61**, 10 417 (2000).
[22] O. Yu. Kolesnychenko, Ph.D. thesis, University of Nijmegen, 2002.
[23] J.H.A. Hagelaar, J.M. Wulveryck, C.F.J. Flipse, E. Bitzet, and P. Gumbsch (private communication).